

On the number and spacing of faults

Chiara Morellato,¹ Francesco Redini² and Carlo Doglioni¹

¹Dipartimento di Scienze della Terra, P.le A. Moro 5, 00185 Roma, Italy; ²Dipartimento di Scienze della Terra e Geologico – Ambientali, Università di Bologna, Via Zamboni 67, 40127 Bologna, Italy

ABSTRACT

Orogens and rift zones have a finite number of regional faults. The accretionary prisms analysed here have a number of thrusts < 50, whereas extensional areas have a number of normal faults ranging between six and 44. The average spacing of thrusts is between 5 and 25 km; spacing of normal faults is more restricted into two peaks, at 25–29 km and 4–6 km, in which the latter is the most common. The number and spacing of faults appear to be mainly controlled by the depth of the decollement plane, which seems to be more variable in

compressive settings with respect to rift zones. Basement-involved orogens present fewer and more spaced thrusts; by contrast, a greater number of thrusts with shorter spacing characterize thin-skinned thrust belts. The shallower the decollement is, the stronger it appears to control the palaeogeography, in the sense of rheological lateral variations in the sedimentary cover.

Terra Nova, 15, 315–321, 2003

Introduction

An issue not sufficiently addressed in the literature is the basic number of tectonic features that develop in different geodynamic settings. The aim here is preliminarily to investigate the number and spacing of faults in thrust belts or extensional basins, and to infer which are the main controlling factors. Measured spacing is then compared with theoretical and experimental predictions to allow consideration of the different accommodation of deformation. We consider here only those faults of regional importance, i.e. faults with more than 100 m offset, faults visible in seismic lines or included in geological sections and maps at scale equal to 1 : 50 000. Several experiments on analogue sandbox models (Mulugeta, 1988; Colletta *et al.*, 1991; Cotton and Koyi, 2000) have shown the importance of the depth and friction of the decollement level in the mechanisms of formation of an accretionary prism. In the presence of a high basal friction, shortening is accommodated by several short-lived steeply dipping thrusts, closely spaced and merged in a narrow zone, producing steep wedges with a high structural elevation. If the decollement level is weak, as with a ductile layer such as provided by evaporites or mudstones, there are few more spaced,

low-angle, long-lived thrusts that generate wider and lower wedges (e.g. Mitra, 1986; Koyi *et al.*, 2000). If the compressive front propagates on a heterogeneous substratum, the models show the formation of non-cylindrical structures, and the transition between different deformation styles generates inflections subparallel to the shortening direction, confined in narrow zones over the boundary between rheologically different decollement levels, represented by a lateral ramp. Wu and Pollard (1995) proposed an experimental study on joint spacing and layer thickness, and Spadini and Podladchikov (1996) have shown a relationship between lithospheric fault spacing and the effective elastic thickness in an elastic plate model of the lithosphere. Lavier *et al.* (2000) analysed numerical experiments of extension, showing that the two types of faulting behaviour depend on brittle layer thickness and cohesion. Ackermann *et al.* (2001), in experimental models, discussed the relationship between fault spacing, length, thickness and percentage extension. They also observed the fractal behaviour of faults at the upper and lower bounds, and its variations in relation to the elastic thickness and the amount of extension.

Methods

We used seismic lines, regional geological profiles, satellite images and maps to measure geometrical characteristics of faults located in several orogens and rift zones of the world, with particular relevance to the

Apennines–Tyrrhenian system. The list of profiles used here (Fig. 1) is given in Tables 1 and 2, respectively, for compressional and extensional settings.

The difference in scale may be a problem because sections at greater scale show only those faults that are of regional importance, whereas those at lower scale are generally more detailed, displaying also lower order structures. A possible solution to this problem would be considering only 'main faults', but their choice would introduce a factor of subjectivity. We therefore decided to consider all the faults with offsets appreciable at the scale of the section (> 100 m), relying on statistics to filter out the noise and to highlight significant patterns. On each section we measured number (N_f) and spacing (S_f) of normal and reverse faults as shown in Figs 2 and 3. Thrust fault spacing was measured on cross-sections (retrodeformed when possible) along continuous regional markers (we usually have chosen the deepest and oldest marker present in each section, e.g. the evaporitic layers in the Apennines, Fig. 2a), considering only faults offsetting such markers. Spacing of normal faults was measured at the surface both in cross-sections and in satellite images because uniform information regarding stratigraphic markers was not available for all sections. Referring to spacing, we calculated the mean values of each profile and of each area, in order to obtain another comparative parameter for the different domains (Fig. 4 and Tables 1 and

Correspondence: Carlo Doglioni, Dipartimento di Scienze della Terra, Università La Sapienza, P. le A. Moro 5, Box 11, 00185 Roma, Italy. E-mail: carlo.doglioni@uniroma1.it

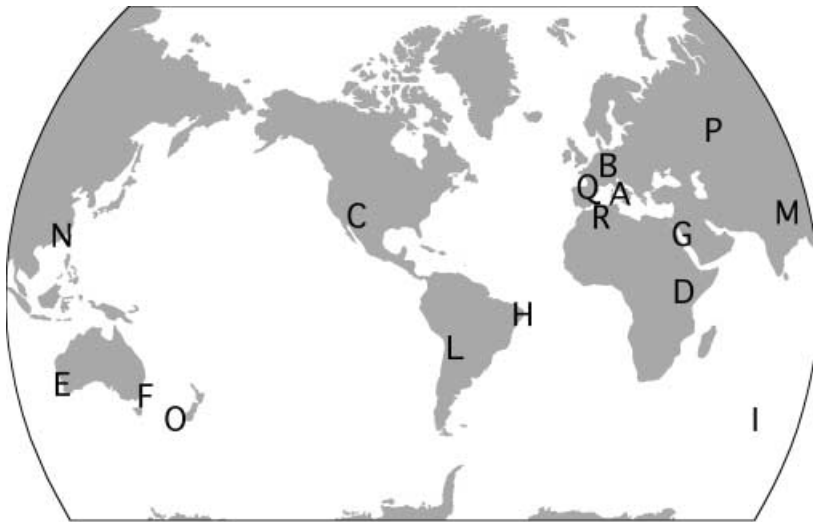


Fig. 1 Location of the investigated areas. Thrust faults: A, Apennines system, Sicily, Alps; L, Bolivia, Andes; M, Nepal; N, China, Taiwan; O, New Zealand; P, Urals; Q, Pyrenees; R, Atlas. Normal faults: A, Tyrrhenian and Pantelleria rifts; B, Rhine graben; C, Basin & Range; D, East African rift; E, Australia 1; F, Australia 2–3; G, Gulf of Suez; H, Brazil; I, Indian Ocean.

2). Note that in order to compute the average spacing between faults (Average S_f), the number of spacings is the number of faults minus one ($N_f - 1$, e.g. 10 faults and nine spacings). For each section we counted the number of faults and normalized this value to the length of 50 km, N_{n50} (Tables 1 and 2). This parameter can be interpreted as a sort of ‘density’ of faults, allowing us to highlight analogies or differences in this distribution, creating a ‘homogeneous’ database independent of the palaeogeographical domain and the scale and length of the profiles (e.g. the Mesozoic Umbro-Marchigiano basin, UM, and the coeval Latium carbonate platform, LA, in the Apennines). The value N_{n50} is computed according to $(N_f \times 50)/\text{Length of the profile}$.

The following areas have been analysed, some of them evidencing both extensional and compressional characteristics:

- 1 Compressional areas: Apennines–Tyrrhenian system, Sicily, Alps, Bolivia, Ural Mountains, New Zealand, Pyrenees, Andes, Nepal, China, Taiwan, Atlas Mountains.
- 2 Rift areas: Apennines–Tyrrhenian system, Basin and Range province, Rhine graben, African Rift, Suez Gulf, Australia (three different areas), Pantelleria area, eastern Brazil, southern Indian Ocean.

The analysed areas are situated in different geodynamic settings in order to study the variations as a function of the tectonic style, the inherited rheology, depth of the decollement planes, crustal and lithospheric thickness, variable heat flow, etc.

Results and conclusions

Counting faults may appear trivial. However, this research shows there are critical and relatively small numbers of regional faults (< 50) in most geodynamic settings. The data (number and average spacing of faults on each section) are shown in Fig. 4 and Tables 1 and 2. Thrust faults have average spacing ranging between 5 and 25 km, without solution of continuity. Two main groups of average spacing values are evidenced in rift systems, related to different types of normal faults (25–29 km, and 4–6 km), regardless of the tectonic setting and crustal thickness. In compressive areas, differences in average thrust spacing are controlled by the variable depth and friction of the decollement planes. In the Apennines, two different groups can be shown in relation to the different inherited rheology from the palaeogeographical setting, e.g. more shale in the Mesozoic basin allowing lower friction in the decollement and wider spacing

between thrust planes. The thrust spacing distribution given in Fig. 4 and Table 1 has an undulating variability for the Apennines, with lower S values at the extremities of the arcs, owing to shorter spacing between thrusts close to thrust belt recesses, which occur along Mesozoic horsts or carbonate platforms.

In comparison, the same measures were made in other compressional settings to highlight differences and analogies between the orogens. The results (Fig. 4) show that the Urals, Taiwan, Atlas Mountains, Pyrenees and New Zealand have values similar to the Apennines, whereas the Alps, Bolivia, Andes, China and Nepal have fewer, but more widely spaced, thrusts. The two main groups differ both in terms of location of the analysed sections relative to the orogen (frontal Vs internal) and in terms of depth of the decollement (relatively shallower and deeper).

Number and average spacing of the normal faults for each section have been compared in the different areas (Fig. 4 and Table 2). A simple frequency analysis of the spacing values has been conducted for each profile in order to determine the main results (Fig. 4). Number of faults is generally higher in back-arc settings (e.g. the Tyrrhenian basin and the Basin and Range). Other parameters are shown in Table 2: the width of grabens (W_g) is generally larger than the width of horsts (W_h). In the Tyrrhenian–Apennines system it should be noted that both W_g and W_h are larger in the southern Tyrrhenian Sea than in the northern Tyrrhenian and onshore, where the back-arc basin is narrower.

Rift zones have the most frequent spacing value of about 5 km, regardless of the rift zone width (compare the number of faults and the width of graben W_g in Table 2).

Fault spacing is more variable for thrusts than for normal faults, in line with the greater variability of the decollement depth in convergent settings: analogue models have demonstrated that decollement depth and friction control the spacing: the deeper the decollement or lower the friction, the larger is the resulting fault spacing (e.g. Colletta *et al.*, 1991). The shallower the decollement is (thin-skinned

Table 1 Database for compressional settings. The length of the profiles is measured at the surface from the first to the last thrust considered, projected if the thrust does not outcrop. Retrodeformed length is the sum of the spacing between thrusts. N_f , number of faults; S_f , spacing between faults; N_{n50} , number of faults normalized to a retrodeformed length of 50 km; Avg N_{n50} , average number of faults for an area normalized to a retrodeformed length of 50 km

Location (average S_f)	Profile name (length)	Retrodeformed length	N_f	Average S_f (km)	N_{n50}	Avg. N_{n50}
Apennines	P09 (51.2 km)	58.8 km	9	7.4	7.6	9
Po Plain (6.2)	P10 (58.9 km)	64.7 km	12	5.9	9.3	
	P11 (58.9 km)	68.4 km	14	5.3	10.2	
N & Central Apennines UM (15.8)	BB1 (170.5 km)	195.5 km	14	15	3.6	3.4
	C03 (136 km)	169.3 km	18	10	5.3	
	BB3 (144.8 km)	312.2 km	24	13.6	3.8	
	BAR (75.9 km)	97.5 km	9	12.2	4.6	
	C&D (64.7 km)	153.7 km	9	19.3	2.9	
	BB4 (157.6 km)	328 km	20	17.3	3	
	BB5 (201.6 km)	385 km	19	21.4	2.5	
	BB6 (284.6 km)	430.5 km	21	21.5	2.4	
	CCPP (111.2 km)	169.1 km	15	12.1	4.4	
Central Apennines LA (11.7)	MM15 (178.5 km)	215.4 km	17	13.5	3.9	4.9
	GVCP (83.3 km)	95.7 km	12	8.7	6.3	
	GVCV (70.7 km)	88.6 km	10	9.8	5.6	
	MM14 (172 km)	167.4 km	11	16.7	3.3	
	MCD2 (57.8 km)	59.1 km	7	9.9	5.9	
	MM13 (118.7 km)	154.8 km	14	11.9	4.5	
S Apennines (7.3)	MRB (61.6 km)	71.6 km	10	8	7	7.2
	MCD (50.2 km)	97.2 km	13	8.8	6.7	
	MRA (103.4 km)	159 km	26	6.4	7.9	
Sicily (10.3)	NRD (63.7 km)	108.9 km	10	12.1	4.6	5.9
	BELLOB (64.1 km)	94.5 km	13	7.9	6.9	
	NRC (67 km)	97.6 km	7	16.3	3.6	
	NRA (54 km)	68.7 km	13	5.7	9.5	
	ANT (132.9 km)	319 km	34	9.7	5.3	
Taiwan (10.2)	Yushing (31.3 km)	42.3 km	5	10.6	5.9	6.1
	Kuanmiao (30.4 km)	39.6 km	5	9.9	6.3	
Atlas (9.4)	Atlas (93 km)	103 km	12	9.4	5.8	5.8
S Urals (10)	Urals (91.6 km)	99.6 km	12	10	6	6
New Zealand (6.6)	NZ (41.5 km)	45.9 km	8	6.6	8.7	8.7
N Pyrenees (7.3)	NPIR (38.5 km)	44 km	7	7.3	8	8
Bolivia (17.2)	LAA' (100 km)	186.4 km	14	14.3	4.2	3.2
	LBB' (67.2 km)	88 km	5	22	2.8	
	KBN (165.4 km)	207 km	11	18.8	2.7	
	KBS (128.7 km)	180 km	11	18	3.1	
	RB3 (43.9 km)	93 km	9	11.3	4.8	
	RB2 (98 km)	209 km	12	19	2.9	
Central Andes (15.2)	Andes (217.6 km)	242.9 km	18	15.2	3.7	3.7
S Alps (20.5)	S.Alps. (90 km)	158.1 km	6	26.4	1.9	3.6
	A.M.S (83.3 km)	117.8 km	8	14.7	3.4	
Nepal (23.6)	Nepal (100 km)	235.6 km	11	23.6	2.3	2.3
China (29.7)	China (79.2 km)	148.5 km	6	9.7	2	2

Sources: Seismic sections P9, P10, P11 (Pieri and Groppi, 1981; northern Apennines); Geological sections BB1, BB3, BB4, BB5, BB6, central–northern Apennines (Bally *et al.*, 1986); CROP 03 (C03) seismic section, central–northern Apennines (Barchi *et al.*, 1998); Geological section E–E' (BAR), central–northern Apennines (Barchi *et al.*, 1999); Geological sections C & D, northern–central Apennines (Calamita and Deiana, 1986); Geological section CCPP, central Apennines (Calamita *et al.*, 1995); Geological sections Cappadocia–Pescara (GVCP) and Canistro–Villalfonsina 1 (GVCV), central Apennines (Vezzani and Ghisetti, 1995); Geological sections MM13, MM14, MM15, southern–central Apennines (Mostardini and Merlini, 1986); Geological sections A–A' (MRA) and B–B' (MRB), southern Apennines (Menardi Noguera and Rea, 2000); Geological sections a (MCD2) and b (MCD), central–southern Apennines (Mazzoli *et al.*, 2000); Geological sections A–A' (NRA), C–C' (NRC), D–D' (NRD), Sicily (Nigro and Renda, 2000); Geological section B, Sicily (Bello *et al.*, 2000); Geological section ANT, offshore western Sicily (Antonelli *et al.*, 1988). Geological sections Yushing and Kuanmyao, south-western Taiwan foreland thrust belt (Mouthereau *et al.*, 2001); Geological section A, Tunisian Atlas (Frizon de

Table 1 (Continued)

Lamotte *et al.*, 2000); Geological section of the Southern Urals (Brown *et al.*, 1997); Seismic section off east coast of North Island, New Zealand (Davey *et al.*, 1986); Geological section of the Northern Pyrenees (Teixell, 1988); Geological sections LAA, LBB, Subandean zone, Bolivia (Leturny *et al.*, 2000); Geological sections KBN, KBS, southern Bolivia (Kley, 1996); Geological sections RB3, RB2, Eastern Cordillera, Bolivia (Roeder, 1988); Geological section CC'–DD', Central Andes, north-western Argentina (Coutand *et al.*, 2001); Geological sections of Southern Alps (S. Alps and AMS; Schönborn, 1999; Schmid and Kissling, 2000); Geological section A–A', Western Nepal (De Celles *et al.*, 2001); Geological section of the Kepingtage thrust zone, China (Allen *et al.*, 1999).

Table 2 Database for extensional settings. N_f , number of faults; S_f , spacing between faults; W_h , average width of grabens; W_{h_1} , average width of horsts; N_{n50} , number of faults normalized to a length of 50 km; Avg N_{n50} , average number of faults for an area normalized to a length of 50 km

Location (average S_f)	Profile name (length)	N_f	Average S_f (km)	W_h (km)	W_g (km)	N_{n50}	Avg. N_{n50}
Apennines–Tyrrhenian System (7.7)	T6 (46 km)	6	5.3	4.5	10.1	6.5	8.54
	C03 (217 km)	13	11.6	10.1	16.4	3	
	T3 (40 km)	9	4.2	2.6	7.5	11.3	
	V6 (22.5 km)	6	3.5		30	13.3	
	Mazz.C (87 km)	15	4.8			8.6	
	MS1 (640 km)	44	16.7	15.7	25.7	3.4	
Basin and Range (13.8)	BB' (560 km)	21	28.2	17.7	14.7	1.9	6.26
	CC' (458 km)	19	25.8	12.6	12.6	2.1	
	Carp.AA' (111 km)	19	5.1	6.3	15.5	8.6	
	Carp.L5-5A (78 km)	13	4.15	5.5	11.8	8.3	
	Carp.L6 (82 km)	17	5.7	5.5	12	10.4	
East African Rift (6.3)	Tan.L220 (36.7 km)	8	4.7		79	10.9	8.6
	Tan.L96 (43.5 km)	7	6.8		90	8	
	Tan.L214 (62.6 km)	10	5.6	16.6	70	8	
	Tan.L208 (34 km)	7	3.5			10.3	
	Anza (93.3 km)	13	7.5		92	7	
	Sudan (40.3 km)	10	3.9		36.7	12.5	
	W-Turk. (129.2 km)	10	12.1	3.4	34	3.9	
Rhine Graben (3.3)	Eco.-Dec.N (63 km)	15	3.9		28	13.1	16.7
	Eco.-Dec.S (44 km)	18	2.8			20.4	
Australia 1 (7.8)	Perth 1 (70 km)	11	6.7	4	42.5	7.9	7.3
	Perth 2 (95.4 km)	9	11.1	43.2	51.1	4.7	
	Perth L3 (37.4 km)	7	5.5	4.25	13.8	9.4	
Gulf of Suez (7.7)	Prof. BB' (120 km)	30	3.4			12.5	8.3
	Prof. FF' (97 km)	8	12.1			4.1	
Brazil (8.8)	AA' (119.7 km)	8	13.4	11.8	34.2	3.3	5.42
	BB' (133.9 km)	16	8.1	9.2	23.8	6	
	CC' (141.5 km)	16	9.3			5.7	
	DD' (70.3 km)	8	7.3			5.7	
	EE' (55.1 km)	7	6.2			6.4	
Indian Ocean (7.6)	L. MD 47 (195 km)	20	7.6			5.1	5.1
Australia 2 (13.6)	L. Eyre (166.4 km)	9	13.6			2.7	7
Australia 3 (4.4)	L. BMR (53.2 km)	12	4.4	1.9		11.3	
Pantelleria (15.1)	L.CS01 (290.3 km)	18	15.1			3.1	3.1

Sources: Line T6, central–northern Tyrrhenian Sea (Pascucci *et al.*, 1999); CROP 03, central–northern Apennines (Barchi *et al.*, 1998); Line T3, northern Tyrrhenian Sea (Pascucci *et al.*, 1999); Line V6, Tuscan Apennines (Pascucci *et al.*, 1999); Geological section Mazz C, southern Apennines (Mazzoli *et al.*, 2000); MS 1, Tyrrhenian Sea (Finetti and Del Ben, 1986); Two profiles traced on a Nevada satellite photo (NOAA satellite, 1996 June 16 UT); Profile AA' (two different interpretations), Line 5–5A, Line 6 (Carpenter and Carpenter, 1994); line 220, line 96, line 214, line 208, Lake Tanganyika (Morley, 1988); Anza rift in Kenya (Bosworth, 1992); Ruwaba subbasin in Sudan (Bosworth, 1992); Western Turkana basin in Kenya (Morley, 1999); Section ECORS/DEKORP N (Wenzel *et al.*, 1991); Section ECORS/DEKORP S (Prodehl *et al.*, 1992); Perth 1, 2, 3, Australia (Song and Cawood, 2000); BB' and FF' profile in the Suez Gulf (Patton *et al.*, 1994); profiles A–A', B–B', C–C', D–D', E–E', north-east Brazilian rift system (Darras de Matos, 1992); LMD 47, Indian Ocean (Rotstein *et al.*, 1992); L Eyre and L BMR Australia (Lister *et al.*, 1991); L CS01, Pantelleria Rift (Torelli *et al.*, 1991).

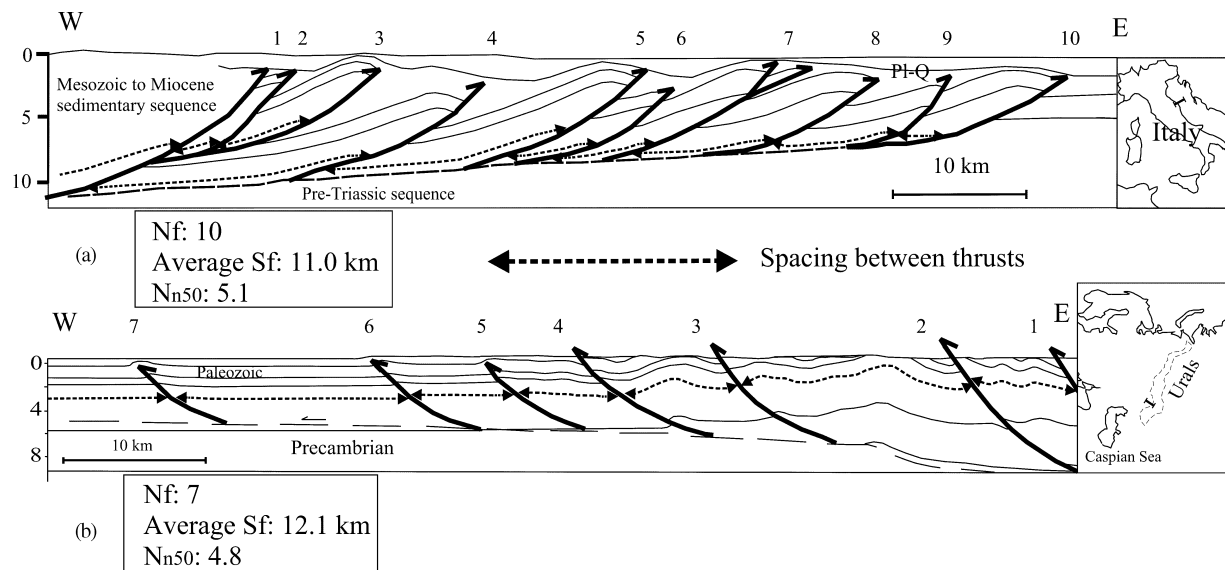


Fig. 2 Examples of measurement in compressional settings. N_f , number of faults; Average S_f , average spacing between faults along the dashed lines; N_{n50} , number of faults normalized to a retrodeformed length of 50 km. (a) Cross-section BB3 in the Apennines area, modified after Bally *et al.* (1986). (b) Cross-section of the southern Urals, modified after Brown *et al.* (1997). See Table 1 for data of the entire sections.

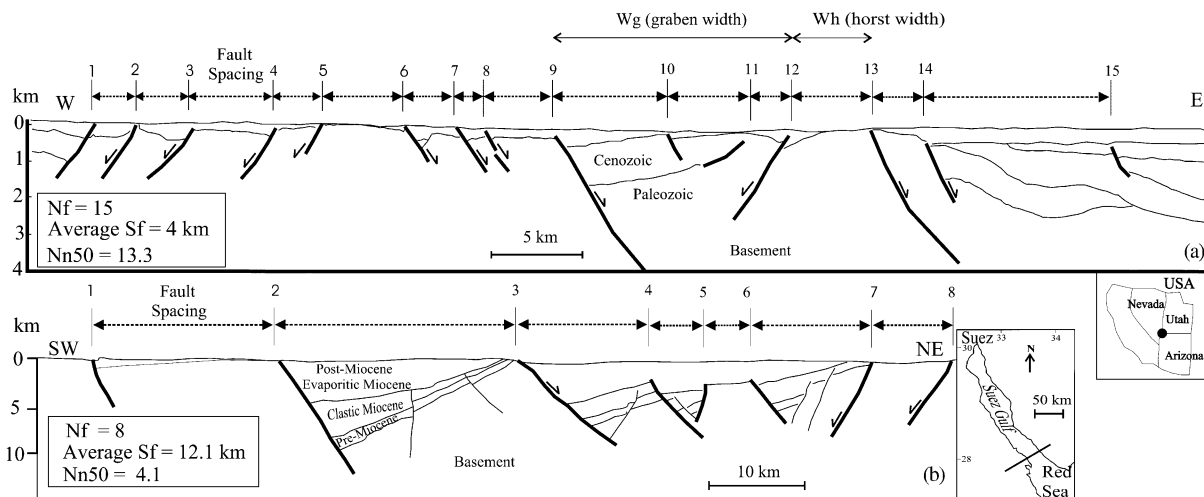


Fig. 3 Examples of measurement in extensional settings. N_f , number of faults; Average S_f , average spacing between faults; N_{n50} , number of faults normalized to the length of 50 km; W_h , horst width; W_g , graben width. (a) Cross-section 6 in the Basin and Range Province, modified after Carpenter and Carpenter (1994); (b) geological profile F-F', in Suez Gulf, modified after Patton *et al.* (1994). See Table 2 for the data of the entire sections.

tectonics), the stronger it appears to control the palaeogeography, in the sense of rheological lateral variations in the sedimentary cover.

In the Apennines, thrusts mainly involve the sedimentary cover (thin-skinned), and the spacing of thrust faults is strongly influenced by palaeogeography and geologically inherited conditions; normal faults, by contrast, appear more independent of the inherited sedimentary cover, possibly owing

to their deeper (thick-skinned) decollement (Bigi *et al.*, 2002).

We are aware that this research needs further investigation both in terms of the quality of the database and the mechanical interpretation of the number and spacing of faults. However, even in a more refined collection of data, the number and spacing of faults are useful parameters because: (i) they provide a tool to predict at which distance new

faults might generate in seismically active areas; (ii) they allow us to infer where to look for unmapped faults; and (iii) they allow us to search for buried faults with hydrocarbon potential. Moreover, these data indicate that continental deformation has a finite number of regional faults, which is related to the thickness of the brittle crust and its mechanical behaviour (e.g. Ackermann *et al.*, 2001).

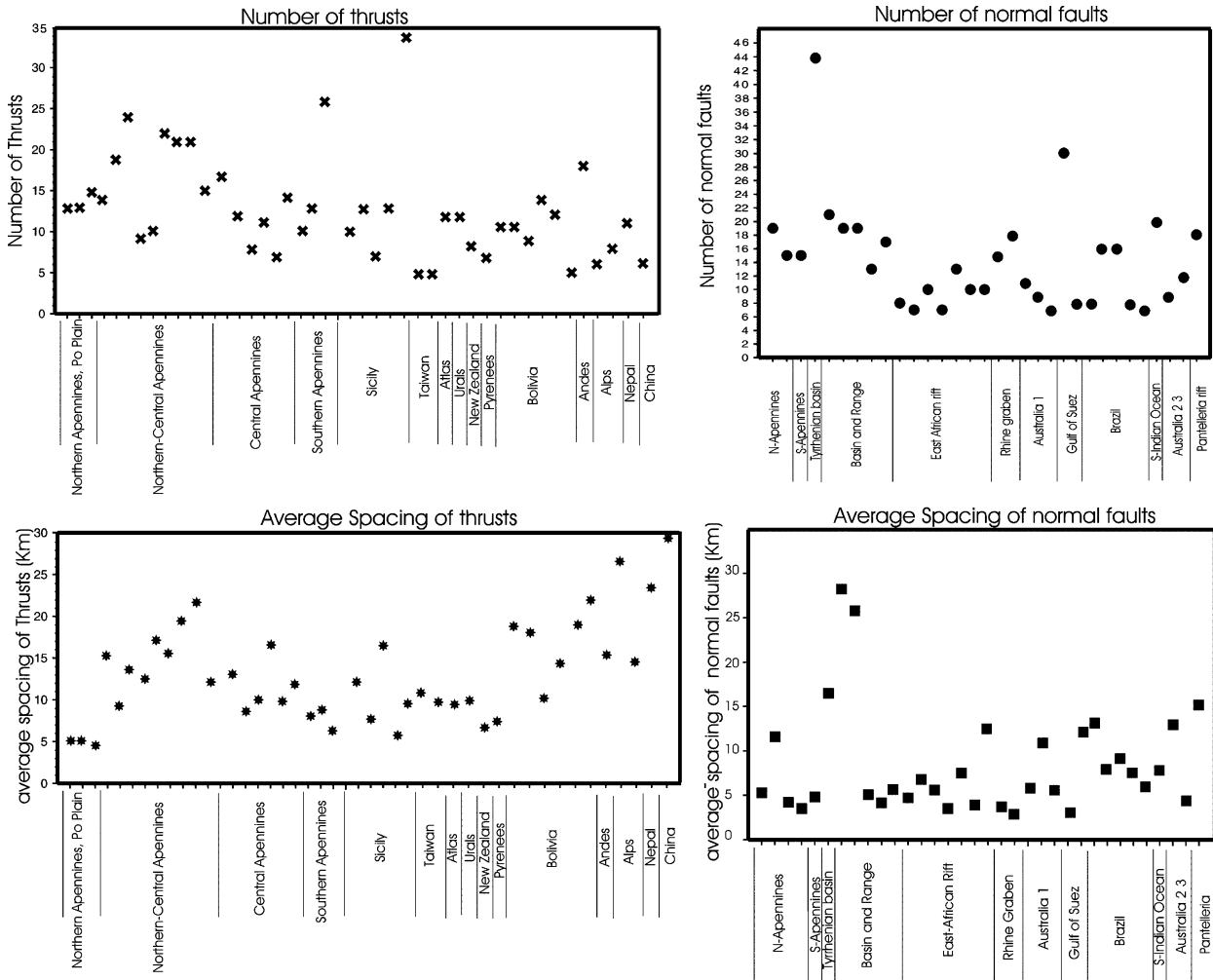


Fig. 4 Number and average spacing of thrusts and normal faults in the studied profiles.

Acknowledgements

Reviews from A. Bally and an anonymous referee were helpful in improving an earlier version of this paper. Comments and discussions with S. Bigi, E. Carminati, G. Mariotti and D. Scrocca are gratefully acknowledged. This research was supported by Cofin 2001, CNR 2000 and ASI 2001.

References

Ackermann, R.V., Schlische, R.W. and Withjack, M.O., 2001. The geometric and statistical evolution of normal fault systems: an experimental study of the effects of mechanical layer thickness on scaling laws. *J. Struct. Geol.*, **23**, 1803–1819.
 Allen, B.M., Vincent, S.J. and Wheeler, P.L., 1999. Late Cenozoic tectonics of the Kepingtage thrust zone interactions of the Tien Shan and Tarim Basin, northwest China. *Tectonics*, **18**, 639–654.

Antonelli, M., Franciosi, R., Pezzi, G., Querci, A., Ronco, G.P. and Vezzani, F., 1988. Paleogeographic evolution and structural setting of the northern side of the Sicily Channel. *Mem. Soc. Geol. It.*, **41**, 141–157.
 Bally, A., Burbi, L., Cooper, C. and Ghe-lardoni, R., 1986. Balanced cross sections and seismic reflection profiles across the central Apennines. *Mem. Soc. Geol. It.*, **35**, 275–310.
 Barchi, M., De Feyter, A., Magnani, M.B., Pialli, G. and Sotera, M., 1998. Extensional tectonics in the Northern Apennines (Italy): evidence from the CROP 03 seismic reflection line. *Mem. Soc. Geol. It.*, **52**, 527–538.
 Barchi, M., Paolacci, S., Pauselli, C., Pialli, G. and Merlini, S., 1999. Geometria delle deformazioni estensionali recenti nel bacino dell’Alta Val Tiberina fra S.Giustino e Perugia: evidenze geofisiche e considerazioni geologiche. *Boll. Soc. Geol. It.*, **118**, 617–625.

Bello, M., Franchino, A. and Merlini, S., 2000. Structural model of eastern Sicily. *Mem. Soc. Geol. It.*, **55**, 61–70.
 Bigi, S., Doglioni, C. and Mariotti, G., 2002. Thrust vs normal fault decollements in the central Apennines. *Boll. Soc. Geol. It.*, Vol. Spec., **1**, 161–166.
 Bosworth, W., 1992. Mesozoic and early Tertiary rift tectonics in East Africa. *Tectonophysics*, **209**, 115–137.
 Brown, D., Alvarez-Marron, J., Perez-Estaun, A., Gorozhanina, Y., Baryshev, V. and Puchkov, V., 1997. Geometric and kinematic evolution of the foreland thrust and fold belt in the southern Urals. *Tectonics*, **16**, 551–562.
 Calamita, F., Coltorti, M., Pieruccini, P. and Pizzi, A., 1995. Evoluzione geomorfologica e strutturale Plio-Quaternaria dell’Appennino Umbro-Marchigiano tra il preappennino umbro e la costa adriatica, presented at Convegno ‘Geodinamica e tettonica attiva del sistema Tirreno-Appennino’. *Came-*

- rino 9–10 Febbraio 1995, *Riassunti*, **51** (52), 1995.
- Calamita, F. and Deiana, G., 1986. Geodinamica dell'Appennino Umbro-Marchigiano. *Mem. Soc. Geol. It.*, **35**, 311–316.
- Carpenter, J.A. and Carpenter, D.G., 1994. Analysis of Basin-Range and Fold-Thrust Structure, and reinterpretation of Mormon Peak Detachment and similar features as Gravity Slide Systems; Southern Nevada, Southwest Utah, and Northwest Arizona. In: S.W. Dobbs and W.J. Taylor, eds., *Structural and Stratigraphic Investigations and Petroleum Potential of Nevada*, with special emphasis south of Railroad valley producing trend. Nevada Petroleum Society Conference. Volume II, p. 15–52, Nevada: Nevada Petroleum Society.
- Colletta, B., Letouzey, J., Pinedo, R., Ballard, J.F. and Balé, P., 1991. Computerized X-ray tomography analysis of sandbox models: examples of thin-skinned thrust systems. *Geology*, **19**, 1063–1067.
- Cotton, J.T. and Koyi, H.A., 2000. Modeling of thrust fronts above ductile and frictional detachments: application to structures in the Salt Range and Potwar Plateau, Pakistan. *Geol. Soc. Am. Bull.*, **112**, 351–363.
- Coutand, I., Cobbold, P.R., de Urreiztieta, M., Gautier, P., Chauvin, A., Gapais, D., Rossello, E.A. and Lopez-Gamundi, O., 2001. Style and history of Andean deformation, Puna plateau, northwestern Argentina. *Tectonics*, **20**, 210–234.
- Darros de Matos, R.M., 1992. The Northeast Brazilian rift system. *Tectonics*, **11**, 766–791.
- Davey, F., Childs, J., Lewis, K. and Hampton, M., 1986. Convergent margin off east coast of North Island, New Zealand, Part I and II. In: *Seismic Images of Modern Convergent Margin Tectonic Structure* (R. von Huene, ed.). *AAPG studies in Geology*, **26**, 50–53.
- De Celles, P.G., Robinson, D.M., Quade, J., Ojha, T.B., Garzzone, C.N., Copeland, P. and Upreti, B.N., 2001. Stratigraphy, structure, and tectonic evolution of the Himalayan fold-thrust belt in western Nepal. *Tectonics*, **20**, 487–509.
- Finetti, I. and Del Ben, A., 1986. Geophysical study of the Tyrrhenian opening. *Boll. Geofis. Teor. Appl.*, **28**, 75–155.
- Frizon de Lamotte, D., Saint Bezar, B. and Bracène, R., 2000. The two main steps of the Atlas building and geodynamics of the western Mediterranean. *Tectonics*, **19**, 740–761.
- Kley, J., 1996. Transition from basement-involved to thin-skinned thrusting in the Cordillera Oriental of southern Bolivia. *Tectonics*, **15**, 763–775.
- Koyi, H.A., Hessami, K. and Teixell, A., 2000. Epicenter distribution and magnitude of earthquakes in fold-thrust belts: insights from sandbox models. *Geophys. Res. Lett.*, **27**, 273–276.
- Lavier, L.L., Buck, W.R. and Poliakov, A.N.B., 2000. Factors controlling normal fault offset in an ideal brittle layer. *J. Geophys. Res.*, **105**, 23431–23442.
- Leturny, P., Mugnier, J.L., Vinour, P., Baby, P., Colletta, B. and Chabron, E., 2000. Piggyback basin development above a thin-skinned thrust belt with two detachment levels as a function of interactions between tectonic and superficial mass transfer: the case of the Subandean Zone (Bolivia). *Tectonophysics*, **320**, 45–67.
- Lister, G.S., Etheridge, M.A. and Symonds, P.A., 1991. Detachment models for the formation of passive continental margins. *Tectonics*, **10**, 1038–1064.
- Mazzoli, S., Corrado, S., De Donatis, M., Scrocca, D., Butler, R.W.H., Di Bucci, D., Naso, G., Nicolai, C. and Zucconi, V., 2000. Time and space variability of 'thin-skinned' and 'thick-skinned' thrust tectonics in the Apennines (Italy). *Rend. Fis. Acc. Lincei*, **9**, 5–39.
- Menardi Noguera, A. and Rea, G., 2000. Deep structure of the Campanian–Lucanian Arc (Southern Apennines, Italy). *Tectonophysics*, **324**, 239–265.
- Mitra, S., 1986. Duplex structures and imbricate thrust systems: geometry, structural position, and hydrocarbon potential. *Am. Ass. Petrol. Geol. Bull.*, **70**, 1087–1112.
- Morley, C.K., 1988. Variable extension in lake Tanganyika. *Tectonics*, **7**, 785–801.
- Morley, C.K., 1999. Marked along-strike variations in dip of normal faults – the Lorichar fault, N Kenya: a possible cause for the metamorphic core complexes. *J. Struct. Geol.*, **21**, 479–492.
- Mostardini, F. and Merlini, S., 1986. Appennino centro-meridionale. Sezioni geologiche e proposta di modello strutturale. *Mem. Soc. Geol. It.*, **35**, 177–202.
- Mouthereau, F., Lacombe, O., Defontaine, B., Angelier, J. and Brusset, S., 2001. Deformation history of the south western Taiwan foreland thrust belt: insights from tectono-sedimentary analyses and balanced cross-sections. *Tectonophysics*, **333**, 293–322.
- Mulugeta, G., 1988. Squeeze box in a centrifuge. *Tectonophysics*, **148**, 323–335.
- Nigro, F. and Renda, P., 2000. Un modello di evoluzione tettono-sedimentaria dell'avanzata neogenica siciliana. *Boll. Soc. Geol. It.*, **119**, 667–686.
- Pascucci, V., Merlini, S. and Martini, P., 1999. Seismic stratigraphy of the Miocene–Pleistocene sedimentary basins of the Northern Tyrrhenian Sea and western Tuscany (Italy). *Basin Res.*, **11**, 337–356.
- Patton, T.L., Moustafa, A.R., Nelson, R.A. and Abdine, A.S., 1994. Tectonic evolution and structural setting of the Suez Rift. *Am. Ass. Petrol. Geol. Mem.*, **59**, 9–55.
- Pieri, M. and Groppi, G., 1981. Subsurface geological structure of the Po plain, Italy. *CNR, Pubbl. No. 414 Del Progetto Finalizzato Geodinamica*, 1–23.
- Prodehl, C., Mueller, S.T., Glahn, A., Gutscher, M. and Haak, V., 1992. Lithospheric cross sections of the European Cenozoic rift system. *Tectonophysics*, **208**, 113–138.
- Roeder, D., 1988. Andean-age structure of eastern Cordillera (province of La Paz, Bolivia). *Tectonics*, **7**, 23–29.
- Rotstein, Y., Schlich, R., Munsch, M. and Coffin, M.E., 1992. Structure and tectonic history of southern Kerguelen Plateau (Indian Ocean) deduced from seismic reflection data. *Tectonics*, **11**, 132–134.
- Schmid, S.M. and Kissling, E., 2000. The arc of the western Alps in the light of geophysical data on deep crustal structure. *Tectonics*, **19**, 62–85.
- Schönborn, G., 1999. Balancing cross sections with kinematic constraints: the Dolomites (northern Italy). *Tectonics*, **18**, 527–545.
- Song, T. and Cawood, P.A., 2000. Structural styles in the Perth Basin associated with the Mesozoic break-up of greater India and Australia. *Tectonophysics*, **317**, 55–72.
- Spadini, G. and Podladchicov, Y., 1996. Spacing of consecutive normal faulting in the lithosphere: a dynamic model for rift axis jumping (Tyrrhenian Sea). *Earth Planet. Sci. Lett.*, **144**, 21–34.
- Teixell, A., 1988. Crustal structure and orogenic material budget in the west central Pyrenees. *Tectonics*, **17**, 395–406.
- Torelli, L., Zitellini, N., Argnani, A., Brancolini, G., De Cilia, C., Peis, D. and Tricart, P., 1991. Sezione geologica crostale dall'avampaese pelagiano al bacino di retroarco Tirrenico (Mediterraneo centrale). *Mem. Soc. Geol. It.*, **47**, 385–399.
- Vezzani, L. and Ghisetti, F., 1995. Domini in compressione ed in distensione al retro di fronti del Gran Sasso – M. Picca e del M. Morrone: il ruolo della zona di taglio Avezzano – Bussi (Appennino centrale). *Studi Geol. Camerti, Volume Spec.*, **1995/2**, 475–490.
- Wenzel, F., Brun, J.P. and the Ecores-Dekorp Working Group, 1991. A deep reflection seismic line across the Northern Rhine Graben. *Earth Planet. Sci. Lett.*, **104**, 140–150.
- Wu, H. and Pollard, D.D., 1995. An experimental study of the relationship between joint spacing and layer thickness. *J. Struct. Geol.*, **17**, 887–905.

Received 28 March 2003; revised version accepted 7 July 2003